HIGH-QUALITY $Al_xGa_{1-x}N$ USING LOW TEMPERATURE-INTERLAYER AND ITS APPLICATION TO UV DETECTOR

M. Iwaya[1], S. Terao[1], N. Hayashi[1], T. Kashima[1], T. Detchprohm[2], H. Amano[1,2], I. Akasaki[1,2], A. Hirano[3] and C. Pernot[3,4]

[1]Department of Electrical and Electronic Engineering, Meijo University, 1-501 Shiogamaguchi, Tempaku-ku, Nagoya 468-8502, Japan

[2]High Tech Research Center, Meijo University, 1-501 Shiogamaguchi, Tempaku-ku, Nagoya, 468-8502, Japan

[3]Research and Development Department, Osaka Gas Co. Ltd., 17 Chudoji-Awata-machi, Shimogyo-ku, Kyoto 600-8815, Japan

[4]Invited researcher from Groupe d'Etude des Semiconducteurs, Universite Montpellier II, Place Eugene Bataillon, 34095 Montpellier Cedex 05, France.

ABSTRACT

Low-temperature (LT-) AlN interlayer reduces tensile stress during growth of $Al_xGa_{1-x}N$, while simultaneously acts as the dislocation filter, especially for dislocations of which Burger's vector contains [0001] components. UV photodetectors using thus-grown high quality $Al_xGa_{1-x}N$ layers were fabricated. The dark current bellow 50 fA at 10 V bias for 10 μm strip allowing a photocurrent to dark current ratio greater than one even at 40 nW/cm^2 have been achieved.

INTRODUCTION

Although there is a large lattice mismatch of about 16% between GaN and sapphire substrate, device-quality GaN has been achieved with use of LT-buffer layer [1]. It was soon followed by the success of control of n-type conductivity by Si-doping [2], and achievement of p-type nitride films using Mg as a dopant [3] and the following special treatment [4]. These successes have led to the commercialization of nitride-based near-UV, blue and green light-emitting diodes and violet laser diodes.

There are another new field waiting for us. Optical devices in near-UV to vacuum-UV region are one of the most attractive target. The applications of which are chemical sensing [5], flame detection [6,7], ozone-hole sensing, remote sensing, high-density optical storage, excitation source for phosphors, fine lithography, etc. In order to realize such device applications, thick $Al_xGa_{1-x}N$ films with high-AlN molar fraction x and high-crystalline quality are essential.

There are several reports concerning the crystalline quality of $Al_xGa_{1-x}N$ films. Koide et al. reported that the crystalline quality of $Al_xGa_{1-x}N$ on a sapphire substrate covered with an LT-AlN buffer layer [8] is much improved in comparison with that of $Al_xGa_{1-x}N$ directly grown on sapphire. It is also reported that its crystalline quality progressively worsens with increasing x reported by Itoh [9]. He also reported that the crystalline quality of $Al_xGa_{1-x}N$ could be significantly improved by growing it on a GaN. At the same time, however, crack network generated with high-density if $Al_xGa_{1-x}N$ exceeded its critical thickness. Therefore, it had been quite difficult to achieve crack-free, high-quality and thick $Al_xGa_{1-x}N$ layers with a high AlN molar fraction.

Very recently, we reported that insertion of LT-deposited layer between HT-GaN reduces

threading dislocation density [10,11]. LT-deposited layer inserted between HT-GaN is called the "LT-interlayer" are GaN film with the dislocation density as low as 5×10^6 cm^{-2} has been achieved. This LT-interlayer technique was applied to grow thick $Al_xGa_{1-x}N$. By using this technique, high quality in terms of narrow X-ray diffraction profile and crack-free $Al_xGa_{1-x}N$ with a whole compositional range was achieved [12-14]. The purpose of this work is to understand the relationship between the microscopic structure and the performance of the photodetectors based on these $Al_xGa_{1-x}N$ layers. For the application of flame sensing, the device should be blind to wavelength longer than 280 nm and have sensitivity on the order of 1 nW/cm^2 for shorter wavelength in order to detect only the flame luminescence. Furthermore, the photocurrent to dark current (PC/DC) ratio should be as large as possible in order to prevent misdetection when the dark current level varies due, for instance, to temperature fluctuation. A response speed on the order of a few ms is sufficient for safety application. Although several groups [15,16] have reported on the evolution of photocurrent with optical power, to our knowledge, there had been no discussion on $Al_xGa_{1-x}N$ based UV detector operated under low illumination intensity (< 1 $\mu W/cm^2$) with high PC/DC-ratio. The metal-semiconductor-metal (MSM) structure, with fabrication simplicity and need for only a single active layer, is useful tool for characterizing the quality of the detection layer. The results obtained by using LT-interlayered-$Al_xGa_{1-x}N$ are very promising for the development of UV high sensitivity detectors.

EXPERIMENT

Unintentionally doped $Al_xGa_{1-x}N$ films with were grown by organometallic vapor-phase epitaxy (OMVPE) at pressures around 200 hPa. Trimethylaluminum, trimethylgallium and ammonia were used as source gases. (0001) c-plane sapphire was used as the substrate. Figures 1(a) - 1(e) schematically show the structure of each sample. In all the growth, we used LT-buffer layer between nitrides and sapphire. Thickness of $Al_xGa_{1-x}N$ was fixed around 1 μm. Samples A was single $Al_{0.43}Ga_{0.57}N$ layer, which is the same as that reported by Koide et al. Sample B was $Al_{0.43}Ga_{0.57}N$ grown on HT-GaN, which is the same as that reported by Itoh et al. Sample C and D were $Al_{0.43}Ga_{0.57}N$ and GaN grown on HT-GaN, but the "LT-AlN interlayer" was inserted between them. Sample E was single HT-GaN. This reference sample is the underlying layer in samples B, C and D. The alloy composition x were precisely determined high-resolution X-ray diffraction. $2\theta/\omega$ scans of the (0002) and (20-24) diffractions were used to determine the lattice constants *c* and *a* at room temperature. For details, see ref. 17.

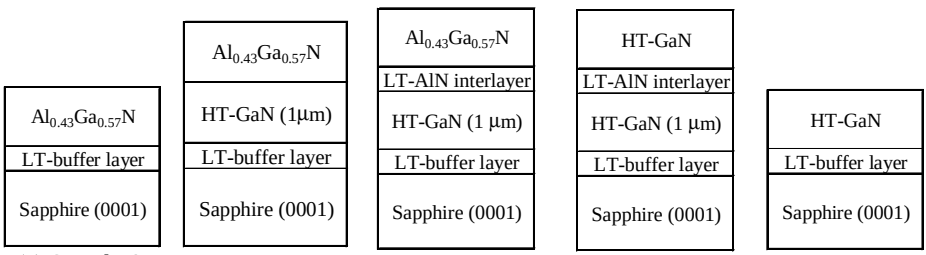

(a) Sample A (b) Sample B (c) Sample C (d) Sample D (e) Sample E

Fig. 1 Structures of the samples.

Plan-view and cross-sectional transmission electron microscopy (TEM) observations were carried out using a HITACHI H-9000NAR TEM system at an acceleration voltage of 300 kV. Ar^+-ion milling and focused Ga^+-ion beam milling were used for plan-view and cross-sectional TEM samples preparation.

The photodetector structure consists of interdigitated electrodes occupying an area of 1 mm^2. The fingers are 10 μm wide with 10 μm spacing. Using a conventional lift-off process, Ti/Au contacts were deposited by electron-beam and thermal evaporation, respectively.

RESULTS AND DISCUSSION

Figures 2(a) through 2(e) show surface SEM micrographs of five samples, respectively. In these five samples, cracks were formed only in sample B. It is identical to the results of Itoh [9]. Although cracks were not generated in sample A, atomic force microscopy showed that the surface was quite rough with a root mean square (RMS) roughness of 12.4 nm. In the image of sample C, which was $Al_{0.43}Ga_{0.57}N$ grown on "LT-AlN interlayer", no cracks are observed. The surface is much smoother than sample A, with the RMS roughness of about 0.4 nm. Both samples D and E are crack-free and have smooth surface.

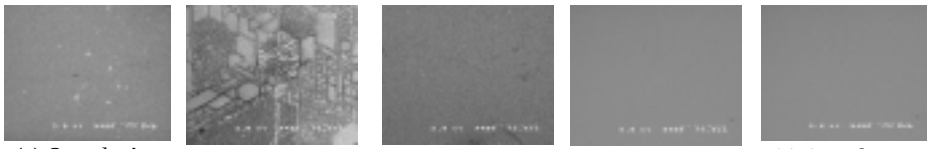

(a) Sample A (b) Sample B (c) Sample C (d) Sample D (e) Sample E

Fig. 2 SEM micrographs of various samples

The mechanism of crack formation was studied by stress observation during growth using multi-beam stress sensor system technique [18]. In case of high-quality crystal, it is found that steep relief of the tensile stress, or in other words crack generation, occurred if thickness*tensile stress product exceeds 0.8 GPa*μm. The tensile stress during growth of $Al_{0.43}Ga_{0.57}N$ on "LT-AlN interlayer" shown as sample C is 0.05 GPa. Therefore, critical thickness is much thicker than 1 μm. In case of $Al_{0.43}Ga_{0.57}N$ grown on GaN shown as sample B, we could not observe the clear strain relief during growth because the critical thickness is too thin. Details was discussed elsewhere [13].

The crystalline quality of two types of crack-free $Al_xGa_{1-x}N$, that is, the same structure of sample A and sample C, is compared. In case $Al_xGa_{1-x}N$ was grown on sapphire using LT-buffer, when the same structure of sample A, the FWHM becomes wider with increasing x, which means the tilting component of the mosaicity increases rapidly with increasing AlN molar fraction. The same tendency has already been reported by Itoh [9]. In constant, when $Al_xGa_{1-x}N$ was grown on "LT-AlN interlyaer", the FWHM of XRC remained unchanged over the entire compositional range. This clearly indicates that the crystalline quality of $Al_xGa_{1-x}N$ film grown on GaN covered with "LT-AlN interlayer" is superior to that grown on sapphire covered with the LT-buffer layer.

Further characterization of the crystalline quality was carried out using TEM. Figures 3(a) and 3(b) show the plan-view TEM images of sample A and C, respectively. Grain boundaries of about 50-250 nm in size were observed in Fig. 3(a). In comparison, such grain boundaries could not be

observed in Fig. 3(b). The structure of $Al_{0.43}Ga_{0.57}N$ shown in Fig. 3(b) is quite similar to that of the underlying GaN except for the density of threading dislocations. When the plan-view image shown in Fig. 3(b) was taken, the sample was slightly tilted from the [0001] axis in order to identify the type of threading dislocations. Using this observation technique, pure-edge and mixed dislocations exhibit strong contrast and can be easily distinguished. For details, see ref. 15. The magnified image in Fig. 3(b) shows that almost all the threading dislocations are pure-edge type ones. The densities of screw and mixed type dislocations are quite low. These results are further confirmed by cross-sectional dark-field image observations. The majority of threading dislocations is in contrast with $\boldsymbol{g}$=[1-100] and out of contrast with $\boldsymbol{g}$=[000-2]. From this result, it is concluded that the majority of threading dislocations in the top $Al_{0.43}Ga_{0.57}N$ layer has Burger's vector $\boldsymbol{b}$=1/3[11-20]. Three types of threading dislocations propagate to the c-direction in hexagonal GaN were reported, that is, screw-type with Burger's vector $\boldsymbol{b}$=[0001], edge-type with $\boldsymbol{b}$=1/3[11-20] and mixed-type with $\boldsymbol{b}$=1/3[11-23]. The results confirmed that the majority of threading dislocations in the uppermost $Al_{0.43}Ga_{0.57}N$ layer is pure-edge-type dislocations. Fig. 4 shows the compositional dependence of the density of threading dislocations in the same structure of sample A and sample C [14].

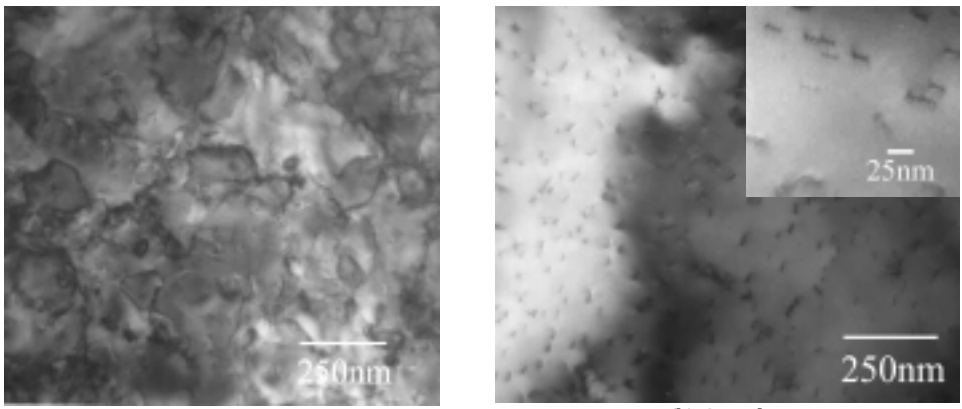

(a) Sample A (b) Sample B

Fig. 3 Bright-field plan-view TEM image of the top surface

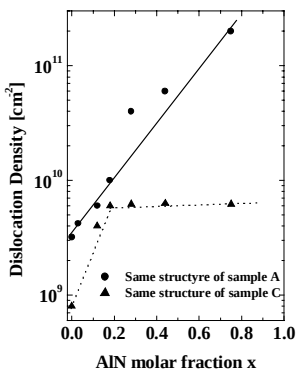

Fig. 4 Compositional dependence of the density of threading dislocations. Solid and dotted lines provide guides for the eye.

Table I. Characteristics of the investigated layers.

sample name	Threading dislocation density [cm^{-2}]				Dark current level at 10V
	edge	screw	mixed	total	
sample A	-	-	-	$> 2\times10^{11}$	~ 40 mA
sample C	$8\text{-}10\times10^{9}$	$< 10^{6}$	$< 10^{7}$	$8\text{-}10\times10^{9}$	< 50fA
sample D	5×10^{8}	$< 10^{6}$	$< 10^{7}$	5×10^{8}	< 50fA
Sample E	$1\text{-}2\times10^{9}$	7×10^{7}	5×10^{8}	2×10^{9}	~ 100 fA

The effects of each type of threading dislocations on the electrical and optical properties have not been clarified yet. Table I summarizes the density of each threading dislocations in these samples. Compared to the underlying GaN layer, $Al_{0.43}Ga_{0.57}N$ grown on "LT-AlN interlyaer" contains higher density of edge type dislocations, although pure screw type and mixed type dislocation is much reduced. In this study, we fabricated and characterized photodetectors based on these four crack-free samples (samples A, C, D and E). Measurements were carried out at room temperature under a bias voltage of 10 V with and without illumination from mercury lamp (λ = 254 nm). The dark current for each sample is listed in Table I. Due to high dark current level, PC/DC of sample A was less than one even for 100 $\mu W/cm^2$. The other samples showed good uniformity from one detector another, and act as high sensitivity UV detectors with PC/DC greater than one even at very low weak illumination of 40 nW/cm^2. Using the mercury lamp at power density of 10 $\mu W/cm^2$ and mechanical shutter, we measured the photoconductive build-up and decay time under 10 V bias at room temperature. Before each experiment, the samples were kept in the dark for at least 12 hours. After the dark current reached a quasi-steady-state value, the excitation light was turned on for 2 hours. When starting measurement, we observed a transient response time as the time needed for the photoresponse signal to drop to 1 % of its maximum value (Fig. 5), compared to the 83 s needed for sample E of HT-GaN grown on LT-AlN buffer layer, samples grown on "LT-AlN interlayer" present much faster decay with response time of 1.6±0.05 s and 2.0±0.1 s, for sample D and C respectively. For sample A, the response time exceeds the measurement time. [7].

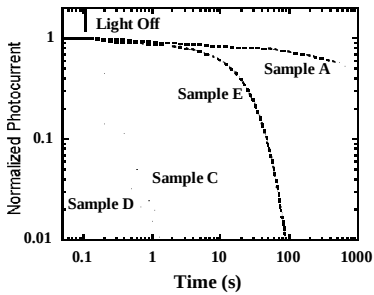

Fig. 5. The normalized photocurrent as a function of time shows a great improvement of the response speed for LT-AlN interlayer.

From these results, it is expected that pure-screw-type and mixed-type threading dislocations are electrically active and relates to deep traps, while pure-edge type dislocation is not so much.

CONCLUSIONS

The relationship between microscopic structure of $Al_xGa_{1-x}N$ and the UV photoconductive properties have been clarified. The "LT-AlN interlayer" is found to act as the dislocation filter, especially for dislocations of which Burger's vector contains [0001] components. The fabricated

MSM detectors show a very low dark-current level, below 50 fA at 10 V. These results show that "LT-interlayered-$Al_xGa_{1-x}N$" are very promising for the development of optical devices in the near-UV and vacuum UV region.

ACKNOWLEDGEMENTS

This work was supported in part by the Japan Society for the Promotion of Science "Research for the Future Program in the Area of Atomic Scale Surface and Interface Dynamics" under the project of "Dynamic Process and Control of the Buffer Layer at the Interface in a Highly-Mismatched System (JSPS96P00204)". and the Ministry of Education, Science, Sports and Culture of Japan, (contract number 11450131).

REFERENCE

1. H. Amano, N. Sawaki, I. Akasaki and Y. Toyoda: Appl. Phys. Lett., **48**, 353 (1986).
2. H. Amano and I. Akasaki: Mat. Res. Soc. Ext Abst., **EA-21**, 165 (1991).
3. H. Amano, M. Kitoh, K. Hiramatsu and I. Akasaki: J. Electrochem. Soc., **137**, 1639 (1990).
4. H. Amano, M. Kito, K. Hiramatsu and I. Akasaki: Jpn. J. Appl. Phys. **28**, L2112 (1989).
5. J. Han, M.H. Crawf, R.J. Shul, S.J. Hearne, E. Chason, J.J Figiel and M. Banas: MRS Internet J. Nitride Semicond. Res. 4S1, G7.7 (1999).
6. C. Pernot, A. Hirano, H. Amano and I. Akasaki: Jpn. J. Appl. Phys.**37**, L1202 (1998).
7. C. Pernot, A. Hirano, M. Iwaya, T. Detchprohm, H. Amano and I. Akasaki: Jpn. J. Appl. Phys. **38**, L487 (1999).
8. Y. Koide, N. Itoh, K. Itoh, N. Sawaki and I. Akasaki, Jpn. J. Appl. Phys. **27**, 1156 (1988).
9. K. Itoh, Doctor Thesis, School of Eng., Nagoya University, Nagoya, 1991.
10. M. Iwaya, T. Takeuchi, S. Yamaguchi, C. Wetzel, H. Amano and I. Akasaki: Jpn. J. Appl. Phys. **37**, L316 (1998).
11. H. Amano, M. Iwaya, T. Kashima, M. Katsuragawa, I. Akasaki, J. Han, S. Hearne, J. A. Floro, E. Chason and J. Figiel, Jpn. J. Appl. Phys. **37**, L1540 (1998).
12. H. Amano, M. Iwaya, N. Hayashi, T. Kashima, M. Katsuragawa, T. Takeuchi, C. Wetzel, I. Akasaki: MRS Internet J. Nitride Semicond. Res. **4S1**, G10.1 (1999).
13. M. Iwaya, S. Terao, N. Hayashi, T. Kashima, H. Amano and I. Akasaki: submitted to Appl. Surf. Sci.
14. T. Kashima, R. Nakamura, M. Iwaya, H. Kato, S. Yamaguchi, H. Amano and I. Akasaki: to be publised Jpn. J. Appl. Phys.
15. E. Muñoz, J. A. Garrido, I. Izpura, F. J. Sánchez, M. A. Sánchez-Garcia, E. Calleja, B. Beaumont and P. Gibart: Appl. Phys. Lett. **71**, 870 (1997).
16. F. Binet, J. Y. Duboz, E. Rosencher, F. Scholtz and V. Härlle: Appl. Phys. Lett. **71**, 1202 (1996).
17. H. Amano, S. Sota, T. Takeuchi, M. Kobayashi, I. Akasaki, J. Burm, W. J. Schaff and L. F. Eastman: Technical Report of IEICE, ED97-123, CPM97-110, 31 (1997-10).
18. J. Floro, E. Chason, S. Lee, R. Twesten, R. Hwang and L. Freund: J. Elec. Mat. **26**, 969 (1997).